momenta to the s lines, selected one each from the s classes R. The assignment of all momenta is complete and it remains to prove that we only need open some or all of these n lines to exhibit every possible divergence. We notice now that for this case the lines (b) acquire an additional property. By counting the lines and vertices we can show that at each vertex there are precisely two lines (a) and not more than one line (b). (We are here dealing with graphs with 3-vertices only), and also there are in all just $(n-1)$ lines (b). If we open one of these lines (b), the graph still remains "connected." Lines (a) defined for the original graph retain their property of splitting graphs even for the new graph; therefore, there are already two (a) lines at each vertex of the new graph. We have seen that at any vertex there cannot be more than two (a) lines. This shows that the (b) lines of the original graph remain the (b) lines of the new graph. The "connectedness" of the graph no longer depends on the lines (b); in other words, lines (b), which were defined in the first place on account of their property of leaving the graph connected if opened one at a time, acquire the further property that they still leave the graph connected if more than one of them are opened simultaneously.[11] The result of opening any set of these lines will therefore never be a divergent part. All divergent parts of the graphs are thus exhibited by opening one or more of lines (a); analytically, this assignment of basic momenta will insure that the entire number of divergences in the graph never exceeds the possible subintegrations at our disposal, and therefore the lemma is proved.

The uniqueness of $I_c(t_1t_2\cdots t_n)$ for a different "correct" choice of basic momenta follows immediately from the concept of classes. For the case dealt with above, the choice is correct only if the basic lines are selected one each from a class R. Since all other lines in a class acquire momenta $p+t$, if t is the basic line which belongs to R, all "correct" choices are completely equivalent, and obtainable one from the other by trivial transformations involving only linear sums of external momenta (p). This proves the result.

We will not deal in detail here with the proof of Lemma 1 for the case of $s<n$ where some at least of the $(n-1)$ fold integrations are "superficially" convergent. The proof requires formulation of rules for assignment of the remaining $(n-s)$ moments which is not difficult.

The proofs in this section, though tedious, are essential because it is important to realize that a subtraction procedure is worthless unless it can be shown that it leads to unique absolutely convergent results.

The author is indebted to Dr. P. T. Matthews and Dr. Res Jost for help in Sec. III and to Professor J. R. Oppenheimer for the very kind hospitality of the Institute for Advanced Study.

---

[11] This result is of course not true for $s<n$.

PHYSICAL REVIEW VOLUME 84, NUMBER 3 NOVEMBER 1, 1951

The Absorption Spectrum of GaCl

Franklyn K. Levin* and J. G. Winans
University of Wisconsin, Madison, Wisconsin

(Received April 23, 1951)

The absorption spectrum of GaCl has been measured and analyzed to provide values for molecular constants. The energy of dissociation for the ground state has been determined from a predissociation limit as less than 5.00 volts and probably greater than 4.98 volts.

INTRODUCTION

WHILE studies of the vibrational spectra of molecules formed by the elements from a single column of the periodic table are not uncommon, investigations of the rotational spectra from various elements in one column have been rare. Such a study has been started for the chlorides formed by the elements of column III. An analysis of the rotational structure of the InCl molecule was made by Froslie and Winans;[1] the rotational spectrum of AlCl was analyzed by Holst.[2]

Two previous investigations of the spectrum of GaCl have been made. Petrikalm and Hochberg[3] obtained the vibrational spectrum in absorption in the region from 3220A to 3470A. The dispersion was sufficient to check the isotope shift due to Cl^{35} and Cl^{37}, but not enough to make a vibrational analysis of the bands. Miescher and Wehrli[4] working with somewhat larger spectrographs confirmed the assignment of the spectrum to GaCl and showed that the heads around 3300A belonged to two overlapping systems. Although Miescher and Wehrli made a thorough and accurate vibrational analysis of the three systems obtained in absorption, the dispersion of their instruments was not sufficient to analyze the rotational structure or determine the position of the null lines.

In the present investigation, the spectrum was

---

* Now with Carter Oil Company, Tulsa, Oklahoma.

[1] H. M. Froslie and J. G. Winans, Phys. Rev. **72**, 481 (1947).

[2] W. Holst, Z. Physik **93**, 55 (1935).

[3] A. Petrikalm and J. Hochberg, Z. Physik **86**, 214 (1933).

[4] E. Miescher and M. Wehrli, Helv. Phys. Acta **7**, 331 (1934).

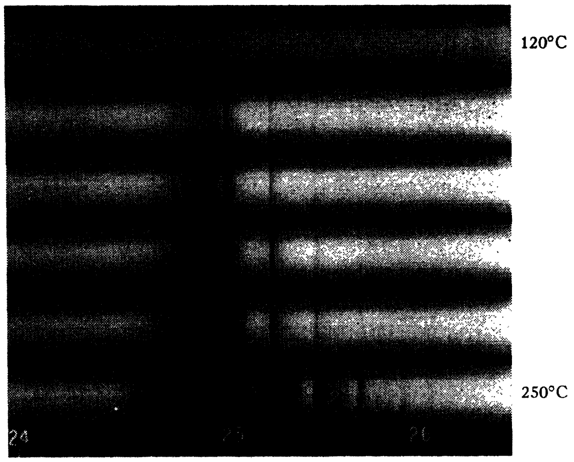

FIG. 1. Spectrum of system *C* of GaCl.

photographed in the third and fourth orders of the 21-foot Wisconsin grating spectrograph. This instrument has a resolving power 90,000 and a dispersion of 0.88A per millimeter in the third order. The grating is one ruled by R. W. Wood on an aluminum surface to give maximum intensity at 11,000A in the first order.

EXPERIMENTAL PROCEDURE

In this study, two fused quartz absorption cells 10 centimeters long and 2.5 centimeters in diameter were used. For preparing these cells a short Pyrex capsule containing commercial quality anhydrous $GaCl_3$ was placed in a vertical tube attached to the pumping system between the cell and liquid air trap. The cell was evacuated and heated at a temperature of 1100°C for forty-eight hours after a "sticking-vacuum" was obtained.

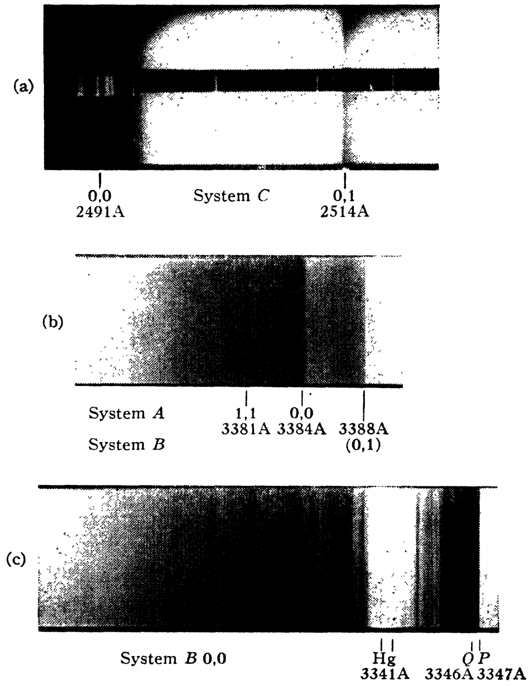

FIG. 2. Bands of GaCl.

When the cell had cooled, a hole was blown in a quartz side tube and a small ball of oxide-free gallium quickly dropped in. The hole was sealed and pumping resumed until a "sticking-vacuum" reappeared. After the heating and evacuation the small capsule containing $GaCl_3$ was broken with a magnetic hammer and some of its contents distilled into the absorption cell by the use of a hand torch. When the cell was sealed off, it contained a small amount of $GaCl_3$ and a piece of gallium metal. At the temperatures used in this experiment, the trichloride was converted to monochloride and the chlorine released reacted with Ga to form more GaCl.

While photographing spectra, the absorption cell occupied the center of a large furnace. A side arm projected into a small second furnace to control the pressure.

In the preliminary absorption experiments, a hydrogen discharge tube was used as a source of continuous radiation. This source was satisfactory for obtaining survey plates with a medium quartz spectrograph. It was, however, not sufficiently intense for use with the grating spectrograph.

The intense continuum between 2570A and 5000A from an H-3 mercury arc was found to be satisfactory. With this source it was possible to photograph two of the band systems of GaCl in either the third or fourth order of the grating spectrograph with an exposure time of three to ten hours. For wavelengths below 2537A, a water-cooled H-6 mercury lamp gave a continuum with intensity such that a fifteen-minute exposure showed the absorption bands between 2480A and 2537A. For the spectral region between 2537A and 2570A where there are many band heads of one of the systems of GaCl, no completely satisfactory light source was available. A Cooper-Hewitt mercury arc operated slightly above the rated power gives a weak continuous background between broadened atomic lines. With exposure times up to eighteen hours, it was possible to obtain about half of the band heads known to exist in the 2537A to 2570A region.

To eliminate the overlapping of orders of the grating spectrograph, the spectral region of interest was separated with a quartz prism between the source and slit.

One of the two quartz absorption cells was also used to obtain the emission spectrum of GaCl. A long wire attached to the tip of a low voltage Tesla coil was inserted into the furnace so that it just cleared the side of the cell.

DESCRIPTION OF SPECTRUM

The emission spectrum after one-hour exposure with the medium quartz spectrograph showed not only the GaCl emission bands but also lines of atomic gallium.

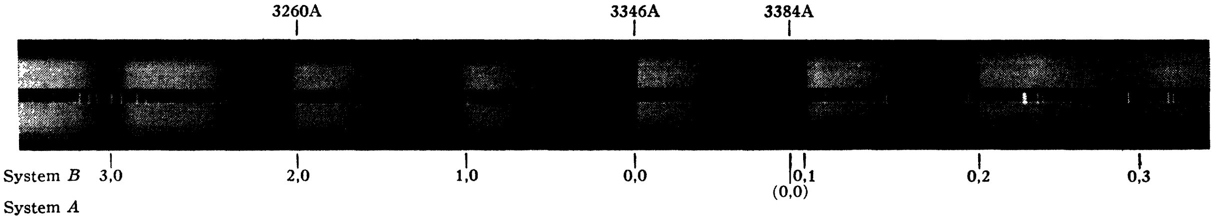

FIG. 3. Systems A and B at $p>5$ atmospheres.

The atomic gallium presumably arose from dissociation of $GaCl_3$ in the discharge.

The general characteristics of the absorption spectrum of gallium chloride are the same as those of indium chloride (reference 1, Fig. 2). The spectrum of system C at pressures corresponding to saturation of $GaCl_3$ from 120°C to 250°C taken with the medium quartz spectrograph is shown in Fig. 1.

A narrow absorption region appears first near 2500A. With increasing temperature and pressure this system broadens toward the red and slightly toward the shorter wavelengths until at a pressure of one atmosphere and at a temperature of 500°C it extends from 2440 to 2760A. The bands in this system are all degraded toward longer wavelengths and alternate bands have sharp double heads. At higher pressures another system of absorption bands appears near 3350A. This consists of six groups of overlapping bands with sharp heads on the long wavelength sides. These bands, extending from 3220 to 3440A, may be arranged as indicated by the isotope shift into two systems.

Two regions of continuous absorption are observed at the higher pressures. The one near 2100A broadens toward longer wavelengths with increasing pressure and the other at 2430A increases in intensity with comparatively little broadening as the pressure is increased. At a pressure of one atmosphere these two continuous regions and the band system from 2440 to 2760 overlap to give continuous absorption from below 2100 to 2610A.

The (0,0) and (1,0) bands of the 2440 to 2760 system in the fourth order are shown in Fig. 2(a) and the (0,0) bands of the two systems near 3300A, in the third order, are shown in Fig. 2(b) and 2(c). The system between 2440 and 2740A consists of a progression of bands with sharp heads alternating with a progression of diffuse bands. Miescher and Wehrli have shown that this system denoted as system C consists of $(0,v'')$ and $(1,v'')$ progressions with (0,0) head at 2490A. The bands with sharp heads form a $(0,v'')$ progression and show no detectable rotational structure other than the sharp heads. The diffuse bands form a $(1,v'')$ progression. In the corresponding system for indium chloride the $(0,v'')$ bands showed rotational structure, the $(1,v'')$ bands showed sharp heads but no other rotational structure, and the $(2,v'')$ bands were diffuse. A few of the strong bands of indium chloride were observed as an impurity spectrum in the absorption spectra of gallium chloride.

The absorption bands between 3220A and 3440A consisting of two overlapping systems were denoted by Miescher and Wehrli as systems A and B. The (0,0) head for the system A is at 3384 and for the system B at 3347A. These are shown in Figs. 2(b) and 2(c). In the present investigation, all of the bands in both systems A and B were found to have rotational structure and several of the bands in system B showed "Q" branches. To ascertain the extent of these systems, some absorption spectra were photographed with a $GaCl_3$ pressure exceeding five atmospheres as determined from the temperature. An example is shown in Fig. 3.

In the emission spectrum, systems A and B appear with high intensity but there is no evidence of any bands of system C. The emission spectrum showed also three sequences of bands degraded toward the red lying between 2370 and 2450, and several additional sequences, also degraded toward longer wavelengths between 2910 and 3210A. It was not possible to obtain enough dispersion or intensity to identify with certainty the molecules responsible for these bands.

ANALYSIS

Vibrational Analysis

The vibrational analysis of the band systems of GaCl made by Miescher and Wehrli[4] was found to be correct both as to the position of the band heads and assignment of quantum numbers. However, since the spectrographs used in the present investigation had higher dispersion, the data are probably more accurate.

A fundamental difficulty in analyzing systems A and B lies in the overlapping of a band of one system by bands belonging to the other system or by the rotational structure of other bands of the same system. Consequently, it was possible to fix the position of the band

TABLE I. Q heads for system B $Ga^{69}Cl^{35}$.

v' \ v''	0		1		2
0	29,873.9 (390.4)	(363.2)	29,510.6 29,512.5[a]	(360.6)	29,150.0 29,153.2[a]
1	30,264.3 30,256.9[b] (379.1)				
2	30,636.0[b]		30,286.6		

[a] $Ga^{71}Cl^{35}$.
[b] $Ga^{69}Cl^{37}$.

TABLE II. Deslandres' table of system A of GaCl.

v''	0		1		2		3		4		5	
v'	Obs.	Calc.	Obs.	Calc.	Obs.	Calc.	Obs.	Calc.	Obs.	Calc.	Obs.	Calc.
0	29,539.0	29,539.0	29,176.1 29,177.8 29,182.6 29,184.2	29,176.2 29,177.8 29,182.4 29,184.1	28,815.5 28,818.9	28,815.7 28,819.0						
1	29,929.5 29,927.6 29,922.3 29,920.5	29,929.5 29,927.6 29,922.3 29,920.3	29,566.6	29,566.6	29,206.1 29,207.8 29,211.9 29,213.3	29,206.2 29,207.6 29,211.9 29,213.4	28,848.1 28,851.4 28,860.6 28,863.4	28,848.2 28,851.3 28,860.4 28,863.5	28,492.4 28,497.2 28,510.5	28,492.6 28,497.4 28,511.0		
2	30,315.3 30,311.7	30,315.3 30,311.5	29,952.5 29,950.4 29,944.8 29,942.8	29,952.4 29,950.4 29,944.8 29,942.8			29,234.1 29,235.3 29,239.8	29,233.9 29,235.3 29,239.2	28,878.0 28,881.5 28,890.0	28,878.3 28,881.3 28,889.9	28,524.6 28,529.3	28,525.2 28,529.8
3			30,333.3 30,329.8 30,319.2	30,333.2 30,329.5 30,319.0	29,972.9 29,970.4 29,965.2 29,963.0	29,972.8 29,970.6 29,965.0 29,963.0					28,906.5 28,909.1 28,917.1	28,906.1 28,909.0 28,917.2
4			30,709.1 30,703.2	30,709.1 30,703.6	30,348.8 30,344.3	30,348.7 30,344.9	29,991.5 29,988.6	29,990.7 29,988.5				
5			31,080.3	31,080.0	30,719.7 30,714.2	30,719.5 30,714.0	30,361.9 30,358.1 30,347.2	30,361.5 30,357.7 30,347.4				
6					31,084.8 31,078.8 31,058.1	31,085.2 31,078.0 31,058.6	30,727.0 30,722.5 30,707.1	30,727.2 30,721.7 30,707.0	30,371.7 30,368.1	30,371.6 30,367.8		
7							31,087.1	31,087.6	30,732.2 30,712.3	30,732.0 30,712.2	30,379.0	30,378.9

head precisely in only a few cases. In general, errors of ±0.1 cm^{-1} were possible. System A arising from a ${}^3\Pi_0 \leftarrow {}^1\Sigma_0^+$ transition (see next section) has only P and R branches while system B representing a ${}^3\Pi_1 \leftarrow {}^1\Sigma_0^+$ transition has P, Q, and R branches. None of the bands was resolved in the neighborhood of the null line, but a few Q heads, which effectively coincide with the null line, could be measured for system B. These are listed in Table I.

Tables II and III are Deslandres' schemes[5] of wave numbers for the band heads of systems A and B. In many cases, heads corresponding to the four isotopic components $\mathrm{Ga^{69}Cl^{35}}$, $\mathrm{Ga^{71}Cl^{35}}$, $\mathrm{Ga^{69}Cl^{37}}$, and $\mathrm{Ga^{71}Cl^{37}}$ were detected and are given in that order. Also listed are values calculated from the formulas:

$$\nu = 29{,}524.3 + \begin{matrix}395.3\\393.4\\388.1\\386.2\end{matrix}(v'+\tfrac{1}{2}) - \begin{matrix}2.3\\2.3\\2.3\\2.2\end{matrix}(v'+\tfrac{1}{2})^2 + \begin{matrix}0.015\\0.015\\0.014\\0.014\end{matrix}(v'+\tfrac{1}{2})^3$$

$$- \begin{matrix}365.3\\363.6\\358.7\\357.0\end{matrix}(v''+\tfrac{1}{2}) + \begin{matrix}1.2\\1.2\\1.2\\1.2\end{matrix}(v''+\tfrac{1}{2})^2$$

for system A and

$$\nu = 29{,}856.3 + \begin{matrix}395.3\\393.4\\388.1\\386.2\end{matrix}(v'+\tfrac{1}{2}) - \begin{matrix}2.5\\2.5\\2.4\\2.4\end{matrix}(v'+\tfrac{1}{2})^2$$

$$- \begin{matrix}365.3\\363.6\\358.7\\357.0\end{matrix}(v''+\tfrac{1}{2}) + \begin{matrix}1.2\\1.2\\1.2\\1.2\end{matrix}(v''+\tfrac{1}{2})^2$$

for system B.

The differences between the experimental and calculated values are less than one wave number. Because of the uncertainty in the position of the heads and because band heads rather than origins were measured, the agreement is satisfactory. Several bands not found by Miescher and Wehrli[4] are included here. In one case [the (1,1) band of system B] a head reported by them proved to be due to a chance coincidence of rotational lines of the (0,0) band.

The coefficients in the formulas for the heads due to $\mathrm{Ga^{71}Cl^{35}}$, $\mathrm{Ga^{69}Cl^{37}}$, and $\mathrm{Ga^{71}Cl^{37}}$ were calculated theoretically from the coefficients found empirically for $\mathrm{Ga^{69}Cl^{35}}$. The agreement between the measured and calculated values shows that there can be little doubt that the bands are due to GaCl.

The band heads measured for system C are listed in Table IV. The heads for the $(0,v'')$ progression could

---

[5] The formulas quoted can be found in Gerhard Herzberg, *Molecular Spectra and Molecular Structure* (D. Van Nostrand, Inc., New York, 1950). All theory necessary for the interpretation can also be found there.

TABLE III. Deslandres' table of system B of GaCl.

v''	0		1		2		3		4		5		6	
v'	Obs.	Calc.	Obs.	Calc.	Obs.	Calc.	Obs.	Calc.	Obs.	Calc.	Obs.	Calc.	Obs.	Calc.
0	29,870.9	29,870.9	29,508.1 29,509.8 29,514.5 29,516.2	29,508.0 29,509.7	29,147.5	29,147.5								
1	30,261.1 30,259.3 30,254.0 30,252.1	30,261.1 30,259.2 30,253.9 30,251.9					29,179.7	29,179.7	28,824.1 28,829.0 28,842.8 28,847.3	28,824.2				
2	30,646.1 30,642.6 30,632.2 30,628.5	30,646.3 30,642.6 30,632.3 30,628.5	30,283.5 30,281.7 30,276.5	30,283.4 30,281.4 30,275.9					29,209.2	29,209.4	28,856.2 28,860.8	28,856.2 28,860.9		
3	31,026.3 31,020.7 31,005.8 30,999.8	31,026.6 31,021.0 31,005.3 31,000.3	30,663.8 30,660.0 30,649.8	30,663.7 30,659.9 30,649.5					29,589.4	29,589.6			28,886.3 28,890.0	28,885.7 28,890.3
4			31,038.8 31,033.4	31,038.8 31,033.3	30,678.8 30,675.1	30,678.4 30,674.6								
5			31,408.5	31,409.0	31,048.7 31,043.4 31,028.6 31,023.0	31,048.6 31,043.0 31,028.2 31,022.6	30,691.7 30,687.2	30,690.5 30,686.7						
6							31,055.8 31,050.6 31,036.0 31,030.7	31,055.7 31,050.2 31,035.6 31,030.0						
7							31,414.6	31,415.8	31,059.9 31,050.6 31,040.9 31,034.8	31,060.2 31,054.8 31,040.6 31,034.9	30,707.1	30,707.1		
8											31,061.3	31,062.2		

be measured accurately. The separations between vibrational states of the ground state may therefore be accurately determined. The wave numbers listed for the $(1,v'')$ progression are those of the centers of the diffuse bands.

Even though the heads of only the $(0,v'')$ progression of system C were known, a method for getting the vibrational constants of the upper electronic state was devised. The wave numbers of the $(0,v'')$ progression can be represented by

$$\nu=\nu_e+\tfrac{1}{2}\omega_e'-\tfrac{1}{4}\omega_e'x_e'-\omega_e''(v''+\tfrac{1}{2})+\omega_e''x_e''(v''+\tfrac{1}{2})^2$$

for Ga^{69}Cl^{35} and

$$\nu^i=\nu_e+\tfrac{1}{2}\rho\omega_e'-\tfrac{1}{4}\rho^2\omega_e'x_e'-\rho\omega_e''(v''+\tfrac{1}{2})+\rho^2\omega_e''x_e''(v''+\tfrac{1}{2})^2$$

for each of the other isotopic combinations. Since system C has the same lower electronic state as systems A and B, ω_e'' and $\omega_e''x_e''$ are known. Thus average values of $\nu_e+\frac{1}{2}\omega_e'-\frac{1}{4}\omega_e'x_e'$ and $\nu_e+\frac{1}{2}\rho\omega_e'-\frac{1}{4}\rho^2\omega_e'x_e'$ can be calculated for the progression. The values so obtained for the three most abundant isotopic combinations give three linear equations to be solved for the unknowns ν_e, ω_e' and $\omega_e'x_e'$. Because the isotopic shift is small and the heads of the less abundant isotopic components weak, the values of $\nu_e+\frac{1}{2}\rho\omega_e'-\frac{1}{4}\rho^2\omega_e'x_e'$ for system C of GaCl showed too much scatter to apply the method successfully.

The values for the separation of the vibrational levels of the lower states as determined from the measurements of heads in systems A, B, and C are listed in Table V. Also listed are the separations calculated from

$$G(v+\tfrac{1}{2})=\begin{array}{c}365.3\\363.6\\358.7\\357.0\end{array}(v''+\tfrac{1}{2})-\begin{array}{c}1.2\\1.2\\1.2\\1.2\end{array}(v''+\tfrac{1}{2})^2.$$

The agreement among the values leaves little doubt

TABLE IV. Deslandres' table for system C of GaCl.

v' \ v''	0	1	2	3	4	5	6	7	8	9
0	40139[a]	39,775.8 39,778.1 39,783.1 39,786.6	39,414.1	39,061[a] 39,078.3 39,083.8	38,703[a] 38,728.8 38,735.6	38,348.0 38,356.7 38,381.6 38,390.4	37,996.7 38,007.3 38,036.2 38,046.9	37,648.8 37,660.7 37,694.9 37,707.4	37,302.7 37,316.7	36,958.9 36,974.5
1	40260[a]				38,820[a]	38,469	38,114	37,760	37,400[a]	37,030[a]

[a] Measured by Miescher and Wehrli. (See reference 4.)

TABLE V. $\Delta G(v+\frac{1}{2})$ for the ground state of GaCl.

v''	System A	System B	System C	Calculated
0	362.8	362.9		362.8
1	360.6	360.5	361.7	360.5
	358.9	359.4		358.8
	353.8	354.0		354.0
	352.4			352.3
2	357.0	358.0		358.0
	356.2	356.4		356.3
		351.3		351.7
		349.9		350.0
3	355.6	355.7		355.6
		354.2		353.9
		350.1	349.5	349.3
			348.2	347.8
4	353.0	353.4		353.1
		352.2		351.5
			347.2	346.9
			345.2	345.4
5			351.3	350.7
			349.4	349.1
			345.4	344.6
			343.5	343.0
6			347.9	348.3
			346.6	346.7
			341.3	341.2
			339.5	340.7
7			346.1	345.8
			344.0	344.2
8			343.8	343.4
			342.2	341.8

that all three systems have the same lower electronic state. The lack of any absorption bands with a ground state different from that for these systems shows that there are no low-lying excited electronic states.

Rotational Analysis

Of the bands shown in Fig. 3, three are sufficiently clear of overlapping structure for rotational analysis. These are the (0,0) and (0,1) bands of system B and the (0,0) band of system A. All are shaded toward shorter wavelengths; hence, all form heads in the P branch.[5] In addition to P and R branches, the bands of system B have Q branches.

System B (0,0) Band

The (0,0) band of system B was the first band analyzed. The Q branch, spreading toward the violet from the Q head, intersects both the R branch and that part of the P branch returning from the head. Alternately, the lines are in phase and not resolved and out of phase and resolved as shown in Fig. 2(c). Beyond this region of poorly defined, broad lines are a series of pairs of lines approximately equally spaced. The stronger member of each pair was found to be a member of the R branch; the weaker, a member of the P branch.

TABLE VI. Calculated values of $\nu_0-\nu_h$.

m (assumed)	$\nu_0-\nu_h$, cm^{-1}
35	4.95
36	3.97
37	3.09
38	2.55

A preliminary numbering of the P and R branches was found by the following procedure. The Q branch can be represented in the first approximation[5] by

$$\nu=\nu_0+eJ(J+1) \qquad (1)$$

where $e=B_{v'}-B_{v''}$. It is found experimentally that e is small so ν_0 can be taken to be at the Q head.

The corresponding equation for the P and R branches is

$$\nu=\nu_0+dm+em^2 \qquad (2)$$

where $d=B_{v'}+B_{v''}$. $m=J+1$ for the R branch, and $-J$ for the P branch, and J is the rotational number for the lower electronic state. The separation between the missing line and head is

$$\nu_0-\nu_h=d^2/4e. \qquad (3)$$

The quantity $\nu_0-\nu_h$ was found by measurement under the assumption that $\nu_0=\nu_{Q\text{ head}}$.

The absolute values of m for the resolved lines in the R branch were not known but the difference of m values for any two R lines could be found by counting. Two equations were formed:

$$\nu_m=\nu_0+dm+em^2 \quad \nu_{m+\Delta m}=\nu_0+d(m+\Delta m)+e(m+\Delta m)^2.$$

A value was assumed for m and then d and e were calculated with $\nu_0=\nu_{Q\text{ head}}$. These values of d and e were next substituted into (3) to calculate $\nu_0-\nu_h$. The assumed value of m was then changed systematically until near agreement with the measured value of $\nu_0-\nu_h$ was attained. The test was very sensitive as shown in Table VI.

The observed value of $\nu_0-\nu_h$ was 2.95 ± 0.10 cm^{-1}. This fixes the correct m as 37. Then considering 3.09 to be the correct value of $\nu_0-\nu_h$, the value of ν_0 was determined. With the numbering known, small changes could be made in the values of the coefficients of (2) to get the best possible fit to all the resolved R branch lines. The semi-empirical formula, with a small cubic correction, is

$$\nu=29{,}873.88+0.3053m+0.00768m^2+0.7\times10^{-6}m^3. \qquad (4)$$

The corresponding values of the molecular constants are

$$B_0'=0.1565\text{ cm}^{-1} \quad\text{and}\quad B_0''=0.1488\text{ cm}^{-1}.$$

With the use of Eq. (4), it was found that a few sharp lines near the Q head belonged to a portion of the P branch with J the same as that in a resolved section of the R branch. Combination differences $\Delta_2F'(J)=R(J)-P(J)$ and $\Delta_2F''(J)=R(J-1)-P(J+1)$ obtained are listed in Table VII.

TABLE VII. Fine structure of some bands of the intercombination systems of GaCl.

Wave numbers of the lines of the bands and the combination differences for these bands.

(0,0) Band of System *A*

J	$R(J)$	$P(J)$	$\Delta_2F'(J)$	$\Delta_2F''(J)$	$\frac{\Delta_2F'(J)}{(J+\frac{1}{2})}$	$\frac{\Delta_2F''(J)}{(J+\frac{1}{2})}$
20	29,552.11					
21	29,552.83					
22	29,553.54					
23	29,554.24					
24	29,554.91					
25	29,555.66					
26	29,556.42					
27	29,557.14					
28	29,557.96					
29	29,558.78					
30	29,559.59					
31	29,560.42			18.77		0.5959
32	29,561.21	29,540.82	20.39	19.35	0.6274	0.5954
33	29,562.17	29,541.07	21.10	19.92	0.6299	0.5946
34	29,563.04	29,541.29	21.75	20.59	0.6304	0.5968
35	29,563.94	29,541.58	22.36	21.15	0.6299	0.5958
36	29,564.88	29,541.89	22.99	21.75	0.6299	0.5959
37	29,565.77	29,542.19	23.58	22.36	0.6288	0.5961
38	29,566.73	29,542.52	24.21	22.95	0.6288	0.5961
39	29,567.72	29,542.82	24.90	23.58	0.6304	0.5970
40	29,568.71	29,543.15	25.56	24.14	0.6311	0.5960
41	29,569.72	29,543.58	26.14	24.67	0.6299	0.5945
42	29,570.72	29,544.04	26.68	25.36	0.6278	0.5967
43	29,571.76	29,544.36	27.40	25.91	0.6299	0.5956
44	29,572.85	29,544.81	28.04	26.47	0.6301	0.5948
45	29,573.91	29,545.29	28.62	27.20	0.6290	0.5978
46	29,575.00	29,545.65	29.35	27.71	0.6312	0.5959
47	29,576.12	29,546.20	29.92	28.24	0.6299	0.5945
48	29,577.20	29,546.76	30.44	28.90	0.6276	0.5959
49	29,578.29	29,547.22	31.07	29.52	0.6277	0.5964
50	29,579.46	29,547.68	31.78	30.02	0.6293	0.5945
51	29,580.67	29,548.27	32.40	30.70	0.6291	0.5961
52	29,581.82	29,548.76	33.06	31.18	0.6297	0.5939
53	29,583.07	29,549.49	33.58	31.78	0.6277	0.5940
54	29,584.29	29,550.04	34.25	32.41	0.6284	0.5947
55	29,585.54	29,550.66	34.88	33.00	0.6285	0.5946
56	29,586.78	29,551.29	35.49	33.58	0.6281	0.5943
57	29,588.04	29,551.96	36.08	34.26	0.6275	0.5958
58	29,589.33	29,552.52	36.81	34.83	0.6292	0.5954
59	29,590.60	29,533.21	27.29	35.39	0.6284	0.5948
60	29,591.97	29,553.94	38.03	35.94	0.6286	0.5940
61	29,593.26	29,554.66	38.60	36.56	0.6276	0.5945
62	29,594.59	29,555.41	39.18	37.11	0.6269	0.5938
63	29,595.98	29,556.15	39.83	37.64	0.6272	0.5928
64	29,597.35	29,556.95	40.40	38.31	0.6264	0.5940
65	29,598.76	29,557.67	41.09	38.94	0.6273	0.5945
66	29,600.18	29,558.41	41.77	39.44	0.6281	0.5931
67	29,601.65	29,559.32	42.33	40.08	0.6271	0.5938
68	29,603.09	29,560.10	42.99	40.70	0.6276	0.5942
69	29,604.61	29,560.95	43.66	41.28	0.6282	0.5940
70	29,606.08	29,561.81	44.27	41.92	0.6279	0.5946
71	29,607.56	29,562.69	44.87	42.50	0.6276	0.5944
72	29,609.06	29,563.58	45.48	43.06	0.6273	0.5939
73	29,610.57	29,564.50	46.07	43.64	0.6268	0.5937
74	29,612.15	29,565.42	46.73	44.19	0.6272	0.5932
75	29,613.71	29,566.38	47.33	44.76	0.6269	0.5928
76	29,615.27	29,567.39	47.88	45.32	0.6259	0.5924
77	29,616.84	29,568.39	48.45	45.88	0.6252	0.5920
78	29,618.46	29,596.39	49.07	46.43	0.6251	0.5915
79	29,620.12	29,570.41	49.72	47.02	0.6254	0.5914
80	29,621.83	29,571.44	50.39	47.66	0.6260	0.5920
81	29,623.47	29,572.47	51.00	48.29	0.6258	0.5925
82	29,625.19	29,573.54	51.65	48.81	0.6261	0.5916
83	29,626.88	29,574.66	52.22	49.47	0.6254	0.5925
84	29,628.60	29,575.72	52.88	50.07	0.6258	0.5925
85	29,630.32	29,576.81	53.51	50.66	0.6258	0.5925
86	29,632.05	29,577.94	54.11	51.21	0.6255	0.5920
87	29,633.83	29,579.11	54.72	51.82	0.6254	0.5922
88	29,635.62	29,580.23	55.39	52.41	0.6259	0.5922
89	29,637.41	29,581.42	55.99	53.01	0.6256	0.5923
90	29,639.24	29,582.61	56.63	53.64	0.6257	0.5927
91	29,641.06	29,583.77	57.29	54.18	0.6261	0.5921
92	29,642.97	29,585.06	57.91	54.82	0.6261	0.5926
93	29,644.77	29,586.24	58.53	55.37	0.6260	0.5922
94	29,646.63	29,587.60	59.03	55.90	0.6247	0.5915
95	29,648.57	29,588.87	59.70	56.50	0.6251	0.5916
96	29,650.49	29,590.13	60.36	57.17	0.6255	0.5924
97	29,652.38	29,591.40	60.98		0.6254	
98	29,654.39			58.37		0.5926
99	29,656.39	29,594.01	62.38		0.6269	
100	29,658.32			59.51		0.5921
101	29,660.22	29,596.88	63.34	60.07	0.6240	0.5918
102	29,662.27	29,598.25	64.02	60.57	0.6246	0.5909
103	29,664.35	29,599.65	64.70	61.28	0.6251	0.5921
104	29,666.35	29,600.99	65.36	61.84	0.6255	0.5918
105	29,668.52	29,602.51	66.01	62.42	0.6257	0.5917
106	29,670.50	29,603.93	66.57	63.08	0.6251	0.5923
107	29,672.51	29,605.44	67.07	63.57	0.6239	0.5913
108	29,674.70	29,606.93	67.77	64.11	0.6246	0.5909
109	29,676.80	29,608.40	68.40	64.81	0.6247	0.5919
110	29,678.93	29,609.89	69.04	65.36	0.6248	0.5915
111	29,681.12	29,611.44	69.68	65.90	0.6249	0.5910
112	29,683.27	29,613.03	70.24	66.55	0.6244	0.5916
113	29,685.52	29,614.57	70.95	67.15	0.6251	0.5916
114	29,687.67	29,616.12	71.55	67.75	0.6249	0.5917
115	29,690.72	29,617.77	72.15	68.32	0.6247	0.5915
116	29,692.16	29,619.35	72.81	68.90	0.6250	0.5914
117	29,694.44	29,621.02	73.42	69.54	0.6249	0.5918
118	29,696.45	29,622.62	73.83	70.08	0.6230	0.5913
119	29,698.99	29,624.36	74.63	70.42	0.6245	0.5892
120	29,701.24	29,626.03	75.21	71.22	0.6241	0.5910
121	29,703.60	29,627.77	75.83	71.77	0.6241	0.5907
122	29,705.98	29,629.47	76.51	72.38	0.6246	0.5909
123	29,708.27	29,631.22	77.05	73.08	0.6239	0.5917
124	29,710.61	29,632.90	77.71	73.58	0.6242	0.5910
125	29,713.01	29,634.68	78.33	74.14	0.6241	0.5908
126	29,715.43	29,636.47	78.96	74.79	0.6242	0.5912
127	29,717.83	29,638.22	79.61	75.46	0.6244	0.5918
128	29,720.32	29,639.97	80.35	75.91	0.6253	0.5907
129	29,722.74	29,641.92	80.82	76.59	0.6241	0.5914
130	29,725.21	29,643.73	81.48	77.13	0.6244	0.5910
131	29,727.67	29,645.61	82.06	77.71	0.6240	0.5910
132	29,730.14	29,647.50	82.64	78.26	0.6237	0.5906
133	29,732.66	29,649.41	83.25	78.80	0.6235	0.5903
134	29,735.18	29,651.34	83.84	79.34	0.6233	0.5899
135	29,737.77	29,653.32	84.45	79.87	0.6232	0.5894
136	29,740.28	29,655.31	84.97	80.63	0.6225	0.5907
137	29,742.87	29,657.14	85.73	81.17	0.6235	0.5903
138	29,745.48	29,659.11	86.37	81.80	0.6236	0.5906
139	29,748.06	29,661.07	86.99	82.37	0.6236	0.5905
140	29,750.70	29,663.11	87.59	82.90	0.6234	0.5900
141	29,753.36	29,665.16	88.20	83.49	0.6233	0.5900
142	29,755.97	29,667.21	88.76	84.09	0.6229	0.5901
143	29,758.58	29,669.27	89.31	84.76	0.6224	0.5907
144	29,761.33	29,671.21	90.12	85.17	0.6237	0.5894
145	29,763.96	29,673.41	90.55	85.79	0.6223	0.5896
146	29,766.67	29,675.54	91.13	86.37	0.6220	0.5896
147	29,769.40	29,677.59	91.81	86.90	0.6224	0.5892
148	29,772.22	29,679.77	92.45	87.47	0.6226	0.5890
149	29,775.00	29,681.93	93.07	88.11	0.6225	0.5894
150	29,777.73	29,684.11	93.62		0.6221	
151	29,780.51			89.31		0.5895
152	29,783.22	29,688.42	94.80	89.79	0.6216	0.5888
153		29,670.72		90.33		0.5885
154		29,692.89				
155		29,695.16				
156		29,697.41				
157		29,699.85				
158		29,702.03				
159		29,704.47				
160		29,706.76				
161		29,709.06				
162		29,711.38				
163		29,713.83				
164		29,716.16				
165		29,718.55				
166		29,720.98				
167		29,723.43				
168		29,725.86				
169		29,728.29				
170		29,730.81				
171		29,733.40				
172		29,735.81				
173		29,738.46				
174		29,740.99				
175		29,743.52				
176		29,746.28				
177		29,748.70				
178		29,751.37				
179		29,753.99				
180		29,756.63				
181		29,759.28				
182		29,761.96				
183		29,764.61				
184		29,767.40				
185		29,770.22				
186		29,772.75				
187		29,775.81				
188		29,778.40				
189		29,781.04				
190		29,783.81				

(0,0) Band of System *B*

J	$R(J)$	$P(J)$	$Q(J)$	$\Delta_2F'(J)$	$\Delta_2F''(J)$	$\frac{\Delta_2F'(J)}{(J+\frac{1}{2})}$	$\frac{\Delta_2F''(J)}{(J+\frac{1}{2})}$
32	29,892.44						
33	29,893.25						
34	29,894.07						
35	29,894.88				21.26		0.5989
36	29,895.72	29,872.81	29,884.05	22.91	21.84	0.6277	0.5984
37	29,896.60	29,873.04	29,884.64	23.56	22.39	0.6283	0.5971
38	29,897.49	29,873.33	29,885.24	24.16	23.01	0.6275	0.5977
39	29,898.35	29,873.59	29,885.92	24.76	23.58	0.6268	0.5970
40	29,899.32	29,873.91	29,886.40	25.41	24.14	0.6274	0.5960

TABLE VII.—*Continued.*

Wave numbers of the lines of the bands and the combination differences for these bands.

(0,0) Band of System *B*

J	$R(J)$	$P(J)$	$Q(J)$	$\Delta_2F'(J)$	$\Delta_2F''(J)$	$\frac{\Delta_2F'(J)}{(J+\frac{1}{2})}$	$\frac{\Delta_3F''(J)}{(J+\frac{1}{2})}$
41	29,900.23	29,874.21	29,887.07	26.02	24.75	0.6270	0.5964
42	29,901.19	29,874.57		26.62	25.36	0.6264	0.5967
43	29,902.17	29,874.87		27.30	25.94	0.6276	0.5963
44	29,903.18	29,875.25		27.93	26.55	0.6276	0.5966
45	29,904.21	29,875.62		28.59		0.6284	
46	29,905.25				27.78		0.5974
47	29,906.11	29,876.43		29.68		0.6248	
48	29,907.25						
49	29,908.33						
50	29,909.45						
51	29,910.60						
52	29,911.73				31.25		0.5952
53	29,912.91	29,879.35		33.56		0.6273	
54	29,914.09						
55	29,915.31						
56	29,916.53				33.61		0.5949
57	29,917.76	29,881.70		36.06	34.28	0.6271	0.5962
58	29,918.86	29,882.25		36.61	34.93	0.6258	0.5971
59	29,920.12	29,882.83		37.29	35.43	0.6267	0.5955
60	29,921.39	29,883.43		37.96	36.07	0.6274	0.5962
61	29,922.65	29,884.05		38.60		0.6276	
62	29,923.96						
63	29,925.26						
64	29,926.54						
			(0,1) Band of System *B*				
15			29,512.64				
16			29,512.86				
18			29,513.46				
19			29,513.79				
21			29,514.52				
22			29,514.85				
23			29,515.16				
27			29,516.78				
28			29,517.28				
29			29,517.81				
30			29,518.27				
31			29,518.74				
32			29,519.33				
33			29,519.92				
34			29,520.42				
36	29,533.14		29,521.43				
37	29,534.01		29,522.03		22.37		
38	29,535.01	29,510.77	29,522.63	24.24	22.90		
39	29,535.90	29,511.11	29,523.36	24.79	23.62		
40	29,536.80	29,511.39		25.41	24.19		
41	29,537.79	29,511.71	29,524.51	26.08	24.71		
42		29,512.09	29,525.22		25.38		
43		29,512.41	29,525.93				
44			29,526.47				
45		29,513.46	29,527.43				
46			29,528.24				
47			29,529.03				
48			29,529.91				
49			29,530.62				
50			29,531.47				
54			29,534.74				
55			29,535.48				
56			29,536.35				
58			29,538.39				

Combination differences for System *B*

(0,0) Band of System *B*

J	$\Delta_1F'(J)=R(J)-Q(J)$	$\Delta_1F'(J)=Q(J+1)-P(J+1)$	$\Delta_1F''(J)=R(J)-Q(J+1)$	$\Delta_1F''(J)=Q(J)-P(J+1)$
35		11.24	10.85	
36	11.67	11.60	11.08	11.01
37	11.96	11.91	11.36	11.31
38	12.25	12.33	11.57	11.65
39	12.43	12.49	11.95	12.01
40	12.92	12.86	12.25	12.19
41	13.16			12.50
		(0,1) Band of System *B*		
36	11.71			
37	11.98		11.38	
38	12.38	12.25	11.65	11.52
39	12.54			11.97
40		12.80	12.29	
41	13.16	13.13	12.57	12.42

For small values of J,

$$\Delta_2F(J)=4B_v(J+\tfrac{1}{2}).$$

Hence, $4B_v$ is the slope of the straight line resulting when $\Delta_2F(J)$ is plotted against J. The values of molecular constants determined from the slopes are

$$B_0'=0.1568\text{ cm}^{-1},\quad B_0''=0.1490\text{ cm}^{-1}.$$

The combination differences for the Q branch lines are

$$\Delta_1F'(J)=R(J)-Q(J)=Q(J+1)-P(J+1),$$

$$\Delta_1F''(J)=R(J)-Q(J+1)=Q(J)-P(J+1),$$

listed in Table VII. The agreement between the two sets of values for $\Delta_1F(J)$ confirms the absolute numbering of the band. The values of $\Delta_1F(J)$ are likely to be less reliable than those of $\Delta_2F(J)$ because the Q "lines" are broad combinations of not quite coincident Q and R or Q and P lines. Using these relations, it was possible to choose from the region of intersecting P, R, and Q branches those lines belonging to the Q branch. The Q branch lines are listed in Table VII.

System B (0,1) Band

The (0,1) band of system B shows only two very small regions clear of the intersecting Q branch. Since the (0,0) and (0,1) bands have a common upper vibrational state, the combination differences $\Delta_2F'(J)$ must be the same for both bands. Some resolved lines near the Q heads were assumed to be P lines and the corresponding R lines calculated from the relation $R(J)=P(J)+\Delta_2F'(J)$, $\Delta_2F'(J)$ being taken from the (0,0) band data. The assumed J was varied systematically until wave numbers calculated agreed with those measured. The numbering was thus established. The values of $\Delta_2F'(J)$ are listed in Table VII. Since there are only four of them, the molecular constants cannot be found by plotting $\Delta_2F(J)$ *vs* J. Since the values of $\Delta_1F'(J)$ were known, from the (0,0) band measurements, the lines belonging to the Q branch of the (0,1) band could be identified. The wave numbers of these lines were plotted against $J(J+1)$, to obtain a line of slope $e=B_0'-B_1''$. The measured value of the slope gave $e=0.0081$. The analysis of the (0,0) band gave $B_0'=0.1568$ cm^{-1}. Hence, $B_1''=0.1487$ cm^{-1}.

To a good approximation, the variation of the rotational constant B_v with vibrational energy is expressible as

$$B_v=B_e-\alpha_e(v+\tfrac{1}{2}),$$

where B_e is the rotational constant in the theoretical vibrationless state and α_e is a constant much less than B_e and characteristic of the electronic state. From values of B_0'' and B_1'' there is obtained $\alpha_e=0.0003$ cm^{-1}.

System A (0,0) Band

The (0,0) band of system A has extensive P and R branches but no Q branch. Near the head, the lines are not resolved and at great distances from the head, the P branch lines become diffuse. Between these regions are a great number of pairs of fairly sharp lines, the weaker of each pair belonging to the head producing P branch. Since there was no Q head, the method of analysis followed for system B could not be used.

Using three among several resolved R branch lines so that the relative rotational quantum numbers were known, the constants for Eq. (2) were calculated for arbitrary values of m. The values of m were then changed until the coefficient $d=(B_0'+B_0'')$ was nearly the same as that found for the (0,0) band of system B. This assumption of nearly equal molecular constants for the two $^3\Pi$ states gave an m numbering good to ± 2. An absolute numbering was then obtained from the requirement that the $\Delta_2F''(J)$ must be the same for this band and the (0,0) band of system B, the lower vibrational state being a common state. The wave numbers and values of $\Delta_2F''(J)$ are listed in Table VII. At $J=77$ an extra line was found both in the P and R branches. This indicates a perturbation in the lower rotational state. The fact that this perturbation was observed for the same value of J in both P and R branches shows that the relative numbering of the P and R branches is correct.

From the plot of $\Delta_2F(J)$ against J, $B_0'=0.1568$ cm^{-1} and $B_0''=0.1485$ cm^{-1}.

The branches extend to sufficiently large values of J to warrant the use of a term in $(J+\frac{1}{2})^3$ in the equations for $F(J)$ and $\Delta_2F(J)$. This term is the correction for the effect of the centrifugal force on the internuclear distance. With this addition

$$\Delta_2F(J)=4B(J+\tfrac{1}{2})-8D(J+\tfrac{1}{2})^3.$$

When $\Delta_2F(J)/(J+\frac{1}{2})$ is plotted against $(J+\frac{1}{2})^2$, there should result a straight line with an intercept $4B$ and a slope $(-8D)$. The values of $\Delta_2F(J)/(J+\frac{1}{2})$ taken from Table VI are plotted against $(J+\frac{1}{2})^2$ in Fig. 4. The values of B obtained from the intercepts and D determined from the slopes are

$$B_0'=0.1568 \text{ cm}^{-1} \qquad B_0''=0.1484 \text{ cm}^{-1}$$

$$D_0'=2.4\times 10^{-8} \text{ cm}^{-1} \quad D_0''=2.4\times 10^{-8} \text{ cm}^{-1}.$$

The experimental points in Fig. 4 deviate markedly from a straight line at low values of $(J+\frac{1}{2})^2$. This same effect appears in the corresponding curves published by Froslie and Winans[1] for InCl. No explanation for this deviation was offered by them nor has one been found in the literature. The function $\Delta_2F(J)/(J+\frac{1}{2})$ is very sensitive at low J values to small changes in wavelength measurements, so that the whole phenomenon may well represent a systematic measuring error.

A determination of the position of the null line was made using the relation

$$R(J-1)+P(J)=2\nu_0+2eJ^2.$$

Let e' be an approximate value so that the true value is $e=e'+\Delta e$. Then $R(J-1)+P(J)=2\nu_0+2e'J^2+2\Delta eJ^2$.

When $R(J-1)+P(J)-2e'J^2$ is plotted against J^2 a straight line results whose intercept gives $2\nu_0$ and slope gives $2\Delta e$. In this way using $e'=0.008$, it was determined that $\nu_0=29{,}542.0$ cm^{-1} and $e=B'-B''=0.00843$ cm^{-1}. The values obtained from combination differences were $e=0.0083$ and 0.0084 cm^{-1}.

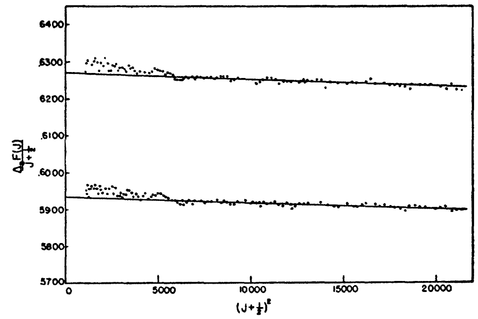

FIG. 4. Plot of $\Delta_2F(J)$ *versus* $(J+\frac{1}{2})^2$ for the (0,0) band of system A of GaCl.

This rotational analysis appears to be satisfactory. The constants found by different procedures agree surprisingly well considering the fact that many of the lines are somewhat diffuse.

ELECTRONIC CONFIGURATION FOR GaCl AND DISSOCIATION ENERGY

The ground state of Ga is $^2P_{\frac{1}{2}}$ and that of Cl is $^2P_{\frac{3}{2}}$. As a chlorine atom in the ground state approaches a gallium atom in the ground state, the molecular states singlet and triplet Σ, Π, and Δ are formed.

If we consider the molecular states to result from the configuration of the $5p$ electrons of the Cl atom and the $1p$ electron of the gallium atom, a closed shell of six electrons $\sigma^2\pi^4$ forms the ground state and this state can be only $^1\Sigma_0{}^+$. The state of next higher energy has electrons $\pi^3\sigma$ giving states $^3\Pi_{2,1,0}$ and $^1\Pi_1$. Of the three band systems observed, system C at 2500A is the most intense in absorption and appears at the lowest pressure. A singlet-singlet transition should be more intense than a singlet-triplet intercombination transition. Hence the system C is considered to be $^1\Pi\leftarrow{}^1\Sigma_0{}^+$ and systems A and B $^3\Pi-{}^1\Sigma_0{}^+$.

Of the three possible systems resulting from $^3\Pi-{}^1\Sigma_0{}^+$, $^3\Pi_2-{}^1\Sigma_0{}^+$ is forbidden by the strict selection rule $\Delta\Omega=0, \pm 1$. Theory further shows that when $\Omega=0$ in both electronic states, the allowed transitions have $\Delta J=\pm 1$ only, giving bands with P and R branches but no Q branch. System A has only P and R branches and therefore must arise from a $^3\Pi_0-{}^1\Sigma_0{}^+$ transition whereas system B which has P, Q, and R branches represents a $^3\Pi_1-{}^1\Sigma_0{}^+$ transition.

The predissociation that occurs in system C makes it possible to fix the energy of dissociation of GaCl within narrow limits. System C is a $^1\Pi_1\leftarrow{}^1\Sigma_0{}^+$ transition, and Kronig's selection rules for predissociation ($\Delta J=0$, $\Delta S=0$, $\Delta\Lambda=0, \pm 1$, $+\leftrightarrow-$, $s\leftrightarrow a$) require that the perturbing state be a $^1\Sigma$, $^1\Pi$, or $^1\Delta$ state. The $^1\Sigma$ state can be eliminated immediately, for it could perturb only one component of the $^1\Pi_1$ state in accordance with the selection rules

$$\Delta J=0 \quad \text{and} \quad +\leftrightarrow-.$$

In such a case, only the P and R branches or the Q

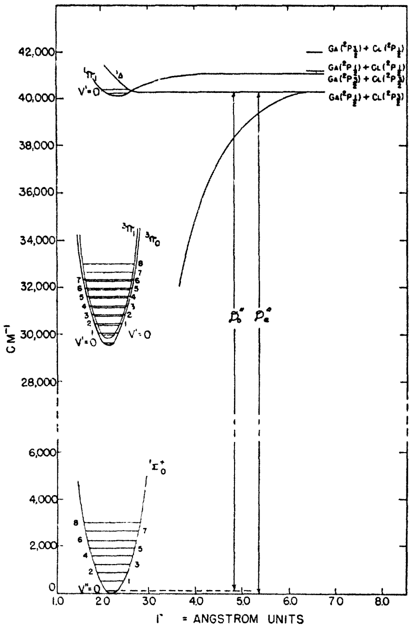

FIG. 5. The potential curves for the low-lying states of GaCl.

branch would be affected. Experimentally, it is found that all branches are missing. A choice between the two remaining possible states $^1\Pi$ and $^1\Delta$ may be made since the narrow continuous absorption band observed at 2430A, appears to represent an absorption from the $^1\Sigma_0{}^+$ ground state into the state causing the predissociation. The selection rule $\Delta\Lambda = 0, \pm 1$ forbids an absorption to a $^1\Delta$ state but permits an absorption to a $^1\Pi$ state. The intensity of this continuous absorption is much less than that of the absorption system C ($^1\Pi \leftarrow {}^1\Sigma_0{}^+$) and corresponds more nearly to that of the forbidden systems A and B ($^3\Pi_{1,0}{}^0 - {}^1\Sigma_0{}^+$). The state causing predissociation could be $^1\Delta$ or $^3\Pi$ depending upon whether the selection rule $\Delta\Lambda = 0, \pm 1$ for absorption is stronger or weaker than the rule $\Delta S = 0$ for predissociation, but it is probably $^1\Pi$. It is shown as $^1\Delta$ in Fig. 5.

Since the state $v' = 0$ for the $^1\Pi$ state of system C shows no rotational structure but the bands have sharp heads, the rotational levels are probably not perturbed at small values of J. Consequently, it is likely that the state $v' = 0$ is stable for low values of J and unstable for higher values of J. The state $v' = 1$ is unstable for all values of J since the bands of this state are diffuse. Potential energy curves are shown in Fig. 5.

The absorption spectrum of GaCl is very similar to that of InCl. For InCl the state $v' = 0$ for system C is stable and rotational structure is observed to values of $J > 100$. The bands with $v' = 1$ for InCl show sharp heads but no other rotational structure and the bands with $v' = 2$ are diffuse. For GaCl, the bands in system C with $v' = 0$ show sharp heads but no other rotational structure and the bands with $v' = 1$ are diffuse. The predissociating limit must therefore either lie between the energies of states $v' = 1$ and $v' = 2$ for InCl and between the energies of $v' = 0$ and $v' = 1$ for GaCl or at an energy not much less than this. This fixes an upper limit to the energy of dissociation as

$$D_0'' = 4.68 \text{ volts for InCl}$$

$$D_0'' = 5.00 \text{ volts for GaCl}$$

with a lower limit not fixed but probably not over about 0.01 volt below 4.66 volts for InCl and 4.98 volts for GaCl. If the predissociation, as is likely, is of the type which sets in rapidly as the energy of the molecule exceeds the energy of the predissociation limit, the values for the dissociation energies are

$$\text{For InCl} \quad D_0'' = 4.655 \pm 0.005 \text{ volts.}$$

$$\text{For GaCl} \quad D_0'' = 4.99 \pm 0.01 \text{ volts.}$$

The very pronounced differences between bands for $v' = 0$, 1, and 2 show that the character of the predissociation changes rapidly with energy.

The possibility that the state causing predissociation has dissociation products different from normal Cl and normal Ga cannot be ruled out. If the dissociation products for this limit are Ga $^2P_{\frac{3}{2}}$ and Cl $^2P_{\frac{3}{2}}$ or Ga $^2P_{\frac{1}{2}}$ and Cl $^2P_{\frac{1}{2}}$, the predissociation should have been more complete since there would be three possible dissociation limits, one at energy about 0.1 volt below the energy of state $v' = 0$.

It is considered unlikely that a stable state such as that of InCl capable of sustaining a rotation of $J > 100$ without dissociating could exist at an energy as much as 0.1 volt above a dissociation limit. The dissociation energies are therefore considered to be most likely those listed above.

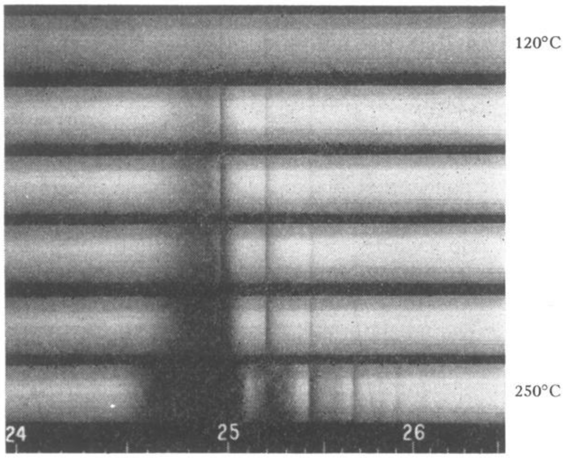

FIG. 1. Spectrum of system *C* of GaCl.

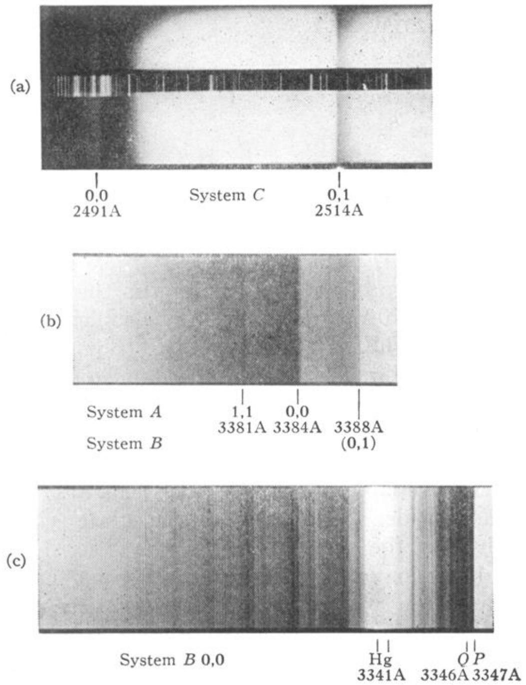

FIG. 2. Bands of GaCl.

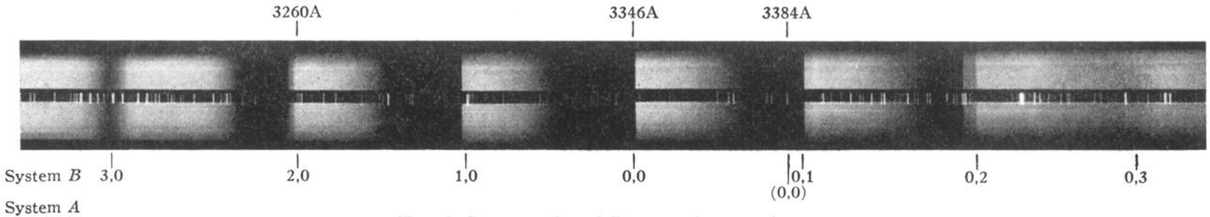

FIG. 3. Systems *A* and *B* at $p > 5$ atmospheres.